

Ferrocene and Maleimide-Functionalized Disulfide Scaffolds for Self-Assembled Monolayers on Gold

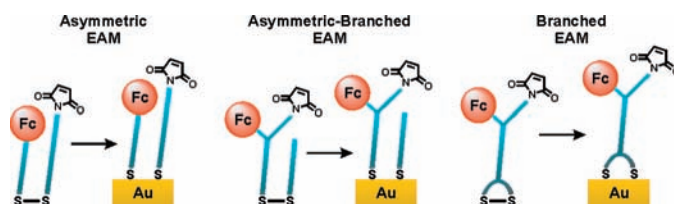
Paul A. Bertin,^{*,†} Michael J. Ahrens,[†] Kinjal Bhavsar,[†] Dimitra Georganopoulou,[†] Markus Wunder,[†] Gary F. Blackburn,[†] and Thomas J. Meade^{*,‡}

Ohmx Corporation, 1801 Maple Avenue, Suite 6143, Evanston, Illinois 60201, and Departments of Chemistry, Biochemistry and Molecular and Cell Biology, Neurobiology and Physiology, and Radiology, Northwestern University, 2145 Sheridan Road, Evanston, Illinois 60208-3113

paul@ohmx.com; tmeade@northwestern.edu

Received May 21, 2010

ABSTRACT



A series of ferrocene-based electroactive molecules (EAMs) containing maleimide and disulfide groups in different asymmetric and branched architectures were designed and synthesized. Stable monolayers of each EAM on gold electrodes were confirmed by cyclic voltammetry. Importantly, these EAMs expand the repertoire of monolayer building blocks amenable to modular biofunctionalization for applications in electrochemical biosensor fabrication.

The anchoring of functional thiol and disulfide molecules to electrodes by way of gold–sulfur interactions provides a powerful yet facile strategy for tailoring interfacial surface properties through the formation of self-assembled monolayers (SAMs).¹ Within this context, electroactive SAMs have emerged as attractive platforms for understanding and manipulating nanoscale charge transfer² with applications ranging from molecular electronics³ and information storage⁴

to cell adhesion⁵ and chemical/biological sensor fabrication.⁶ Consequently, the pursuit of SAM building blocks in the form of organosulfur compounds functionalized with redox-active groups remains an important objective in modern synthetic chemistry.⁷

[†] Ohmx Corporation.

[‡] Northwestern University.

(1) (a) Love, J. C.; Estroff, L. A.; Kriebel, J. K.; Nuzzo, R. G.; Whitesides, G. M. *Chem. Rev.* **2005**, *105*, 1103. (b) Gooding, J. J.; Mearns, F.; Yang, W. R.; Liu, J. Q. *Electroanalysis* **2003**, *15*, 81. (c) Nuzzo, R. G.; Allara, D. L. *J. Am. Chem. Soc.* **1983**, *105*, 4481. (d) Porter, M. D.; Bright, T. B.; Allara, D. L.; Chidsey, C. E. D. *J. Am. Chem. Soc.* **1987**, *109*, 3559.

(2) (a) Eckermann, A. L.; Feld, D. J.; Shaw, J. A.; Meade, T. J. *Coord. Chem. Rev.* **2010**, *254*, 1769. (b) Haddox, R. M.; Finklea, H. O. *J. Phys. Chem. B* **2004**, *108*, 1694. (c) Chidsey, C. E. D.; Bertozzi, C. R.; Putvinski, T. M.; Mujisce, A. M. *J. Am. Chem. Soc.* **1990**, *112*, 4301. (d) Chidsey, C. E. D. *Science* **1991**, *251*, 919.

(3) Shirai, Y.; Cheng, L.; Chen, B.; Tour, J. M. *J. Am. Chem. Soc.* **2006**, *128*, 13479.

(4) Wei, L. Y.; Padmaja, K.; Youngblood, W. J.; Lysenko, A. B.; Lindsey, J. S.; Bocian, D. F. *J. Org. Chem.* **2004**, *69*, 1461.

(5) Yeo, W. S.; Mrksich, M. *Langmuir* **2006**, *22*, 10816.

(6) (a) Beer, P. D.; Davis, J. J.; Drillsma-Milgrom, D. A.; Szemes, F. *Chem. Commun.* **2002**, 1716. (b) Kerman, K.; Mahmoud, K. A.; Kraatz, H. B. *Chem. Commun.* **2007**, 3829. (c) Mahmoud, K. A.; Kraatz, H. B. *Chem.—Eur. J.* **2007**, *13*, 5885. (d) March, G.; Noel, V.; Piro, B.; Reisberg, S.; Pham, M. C. *J. Am. Chem. Soc.* **2008**, *130*, 15752. (e) Ricci, F.; Bonham, A. J.; Mason, A. C.; Reich, N. O.; Plaxco, K. W. *Anal. Chem.* **2009**, *81*, 1608. (f) Xiao, Y.; Qu, X. G.; Plaxco, K. W.; Heeger, A. J. *J. Am. Chem. Soc.* **2007**, *129*, 11896. (g) Yu, C. J.; Wan, Y. J.; Yowanto, H.; Li, J.; Tao, C. L.; James, M. D.; Tan, C. L.; Blackburn, G. F.; Meade, T. J. *J. Am. Chem. Soc.* **2001**, *123*, 11155. (h) Zhi, F. P.; Lu, X. Q.; Yang, J. D.; Wang, X. Y.; Shang, H.; Zhang, S. H.; Xue, Z. H. *J. Phys. Chem. C* **2009**, *113*, 13166.

(7) Witt, D.; Klajn, R.; Barski, P.; Grzybowski, B. A. *Curr. Org. Chem.* **2004**, *8*, 1763.

Our interest in SAMs as electrochemical biosensor platforms prompted an investigation into ferrocene-based electroactive molecules (EAMs) to serve as signal transduction scaffolds amenable to modular biofunctionalization. To this end, we report the synthesis and electrochemical SAM characterization of a series of EAMs that combine ferrocene, maleimide, and disulfide groups in different architectures. Each EAM was designed to facilitate dilute mixed monolayers of ferrocene and maleimide groups in close spatial proximity. Ferrocenes were chosen as model redox probes due to their well-known, reversible electrochemistry in SAMs.⁸ Maleimides were incorporated as cross-linking functional groups to allow for modular immobilization of sulfhydryl-containing biomolecules following monolayer assembly.⁹ Disulfides were employed as gold-anchoring groups due to compatibility with maleimides and to impart the practical advantage of air stability. Importantly, these EAM architectures are generalizable to alternate redox motifs and designed to serve as electrochemical signaling scaffolds for comprehensive studies that probe the influence of biomolecule ligand–receptor interactions on the reorganization energies of transition metal-modified SAMs.¹⁰

Structures of the EAMs (1–5) presented in this work are shown in Figure 1. For each EAM in the series, ferrocene

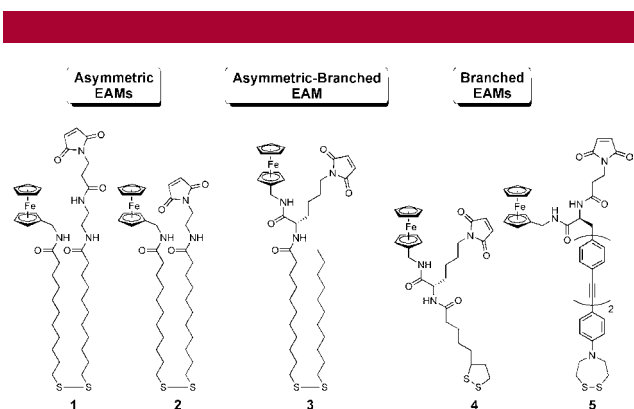


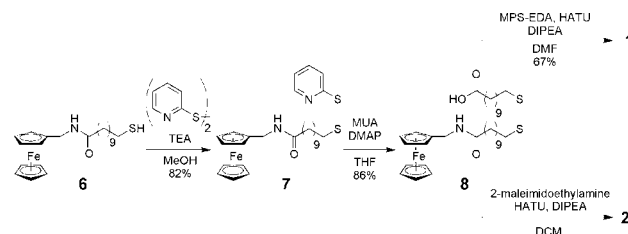
Figure 1. Structures of asymmetric (1–2), asymmetric-branched (3), and branched (4–5) EAMs prepared in this study.

was linked to the disulfide bridging framework via an amidomethyl group to impart a consistent electronic influence on the oxidation potential. EAMs 1 and 2 comprise asymmetric dialkyl disulfides end-functionalized with ferrocene and maleimide groups of different bridge lengths. Asymmetric disulfides are known to produce mixed SAMs with

well-defined surface compositions and have been shown to avoid phase segregation when diluted with symmetric disulfides in some instances.¹¹ Therefore, EAMs 1 and 2 provide a means for preparing dilute SAMs on gold with neighboring ferrocene and maleimide terminal groups in a single incubation step. Alternatively, EAM 3 was designed with ferrocene and maleimide groups arranged as terminal branching groups from a single amino acid-functionalized asymmetric disulfide bridge. The branched headgroup of 3 will ensure nearby ferrocenes and maleimides in dilute SAMs but may alter the surface coverage and packing compared to 1 and 2.¹² Lastly, EAMs 4 and 5 were designed with similar amino acid-branched ferrocene and maleimide headgroups linked to lipoic acid and dithiazepane-capped oligophenylethynyl bridges, respectively. These branched EAM architectures were chosen to provide different bridge lengths and permit bipodal gold anchoring.¹³

The syntheses of asymmetric EAMs 1 and 2 are shown in Scheme 1 and adapted from established asymmetric disulfide

Scheme 1. Syntheses of Asymmetric EAMs 1 and 2



methodology.^{9a} Starting from 11-mercapto-*N*-(ferrocenylmethyl)undecanamide 6,¹⁴ the thiol was treated with 2,2'-dipyridyl disulfide and TEA to yield the pyridyl disulfide derivative 7. Subsequent displacement of the thiopyridyl group with MUA generated the intermediate ferrocenyl asymmetric disulfide 8. The carboxylic acid group of 8 was activated with HATU and coupled to MPS-EDA to yield the target EAM 1. Similar coupling conditions were employed between 8 and 2-maleimidoethylamine to afford EAM 2.

The syntheses of asymmetric-branched EAM 3 and branched EAM 4 proceeded from common precursors as shown in Scheme 2. Aminomethylferrocene 9¹⁵ was coupled to *N*- ϵ -maleoyl- α -Boc-L-lysine 10¹⁶ using HATU to yield the ferrocenyl-maleimide branched subunit 11. Conversion

(8) Finklea, H. O. In *Electroanalytical Chemistry: A Series of Advances*; Marcel Dekker: New York, 1996; Vol. 19, p 109.

(9) (a) Houseman, B. T.; Gawalt, E. S.; Mrksich, M. *Langmuir* **2003**, *19*, 1522. (b) Yeo, W. S.; Min, D. H.; Hsieh, R. W.; Greene, G. L.; Mrksich, M. *Angew. Chem., Int. Ed.* **2005**, *44*, 5480. (c) Wettero, J.; Hellerstedt, T.; Nygren, P.; Broo, K.; Aili, D.; Liedberg, B.; Magnusson, K. E. *Langmuir* **2008**, *24*, 6803.

(10) (a) Barker, K. D.; Eckermann, A. L.; Sazinsky, M. H.; Hartings, M. R.; Abajian, C.; Georganopoulou, D.; Ratner, M. A.; Rosenzweig, A. C.; Meade, T. J. *Bioconjugate Chem.* **2009**, *20*, 1930. (b) Orlowski, G. A.; Chowdhury, S.; Kraatz, H.-B. *Langmuir* **2007**, *23*, 12765. (c) Smalley, J. F.; Feldberg, S. W.; Chidsey, C. E. D.; Linford, M. R.; Newton, M. D.; Liu, Y. P. *J. Phys. Chem.* **1995**, *99*, 13141.

(11) Chen, S. F.; Li, L. Y.; Boozer, C. L.; Jiang, S. Y. *J. Phys. Chem. B* **2001**, *105*, 2975.

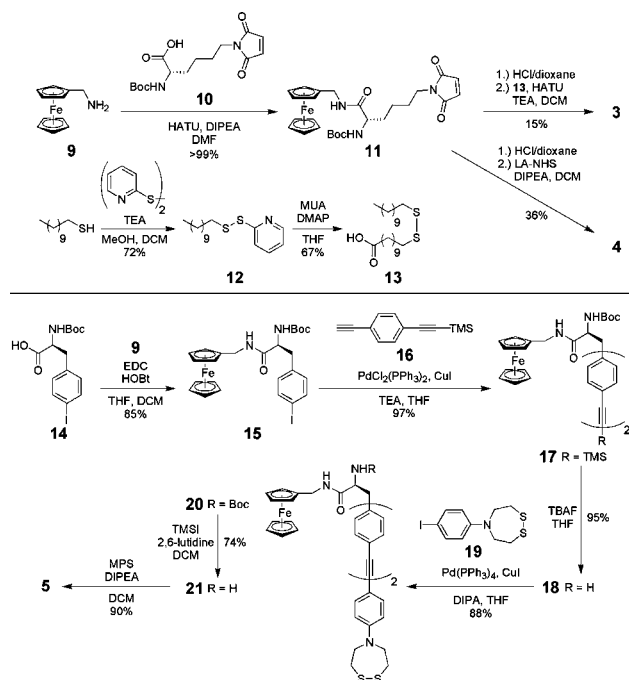
(12) (a) Appoh, F. E.; Kraatz, H.-B. *J. Phys. Chem. C* **2007**, *111*, 4235. (b) Chechik, V.; Schonherr, H.; Vancso, G. J.; Stirling, C. J. M. *Langmuir* **1998**, *14*, 3003.

(13) (a) Bertin, P. A.; Georganopoulou, D.; Liang, T. Y.; Eckermann, A. L.; Wunder, M.; Ahrens, M. J.; Blackburn, G. F.; Meade, T. J. *Langmuir* **2008**, *24*, 9096. (b) Willey, T. M.; Vance, A. L.; Bostedt, C.; van Buuren, T.; Meulenber, R. W.; Terminello, L. J.; Fadley, C. S. *Langmuir* **2004**, *20*, 4939.

(14) Eggers, P. K.; Hibbert, D. B.; Paddon-Row, M. N.; Gooding, J. J. *J. Phys. Chem. C* **2009**, *113*, 8964.

(15) Bublitz, D. E. *J. Organomet. Chem.* **1970**, *23*, 225.

Scheme 2. Syntheses of Asymmetric-Branched EAMs **3** and Branched EAMs **4** and **5**



of 1-undecanethiol into pyridyl disulfide derivative **12** followed by displacement of the thiopyridyl group with MUA yielded asymmetric disulfide anchoring intermediate **13**. Removal of the Boc group in **11** with HCl followed by coupling to **13** with HATU afforded asymmetric-branched EAM **3** in modest yield. Alternatively, **11** was deprotected and treated with LA-NHS¹⁷ and DIPEA to yield branched EAM **4**.

The synthetic procedure for branched EAM **5** began by coupling **9** to *N*-Boc-4-iodo-L-phenylalanine **14** using EDC and HOBT to yield **15** (Scheme 2). Subsequent Pd/Cu catalyzed cross-coupling of **15** with 1-ethynyl-4-(trimethylsilyl)benzene **16**¹⁸ yielded intermediate **17**. Removal of the TMS group from **17** with TBAF afforded **18** which was further coupled with 5-(4-iodophenyl)-[1,2,5]-dithiazepane **19**^{13a} using alternate cross-coupling conditions to yield the ferrocenyl-branched oligophenylethynyl “wire” intermediate **20**. It should be noted that repeated attempts to remove the Boc group in **20** under strongly acidic conditions (HCl or TFA) resulted in decomposition of the conjugated electron-rich wire framework. However, cleavage of the Boc group with TMSI¹⁹ and 2,6-lutidine in DCM proceeded smoothly to afford amine derivative **21**. Further coupling to MPS in DCM with DIPEA yielded the target branched EAM **5**.

(16) Wakisaka, K.; Arano, Y.; Uezono, T.; Akizawa, H.; Ono, M.; Kawai, K.; Ohomomo, Y.; Nakayama, M.; Saji, H. *J. Med. Chem.* **1997**, *40*, 2643.

(17) Liu, W.; Howarth, M.; Greytak, A. B.; Zheng, Y.; Nocera, D. G.; Ting, A. Y.; Bawendi, M. G. *J. Am. Chem. Soc.* **2008**, *130*, 1274.

(18) Huang, S. L.; Tour, J. M. *J. Org. Chem.* **1999**, *64*, 8898.

(19) Lott, R. S.; Chauhan, V. S.; Stammer, C. H. *J. Chem. Soc., Chem. Commun.* **1979**, 495.

Mixed SAMs of EAMs **1–5** were prepared by incubating gold microelectrodes in ethanolic solutions of the respective EAM (0.1 mM) with undecyl disulfide ((C₁₁S)₂, 0.5 mM) and bis(11-hydroxyundecyl) disulfide ((HO-C₁₁S)₂, 0.5 mM) diluents for 18 h. Following extensive washing, the SAMs were characterized by cyclic voltammetry (CV) (see Supporting Information).

Briefly, the CV experiments employed an electrochemical cell with SAM-modified gold as the working electrode (*d* = 0.25 mm), a platinum wire counter electrode, and a silver wire quasi-reference electrode (Ag QRE). Potentials relative to an internal standard redox couple of 1,1'-ferrocene dimethanol were 36 ± 1 mV more negative than those versus Ag QRE. The reported potentials herein are relative to Ag QRE.

Table 1. Electrochemical Properties of EAMs **1–5** in Diluted SAMs on Gold Microelectrodes^a

EAM	E^0 (mV)	ΔE_p (mV)	ΔE_{fwhm} (mV)	i_{pa}/i_{pc}	Γ_{Fc} (x 10 ⁻¹¹ mol·cm ⁻²)
1	87	8	122	0.9	2.73 ± 0.16
2	70	6	112	1.0	2.67 ± 0.28
3	52	11	117	1.0	3.16 ± 0.07
4	62	11	134	1.1	4.80 ± 0.35
5	87	17	108	1.1	6.65 ± 0.14

^a Values reported as averages from three different electrodes. Standard deviations for E^0 and ΔE_p = 1 mV, ΔE_{fwhm} ≤ 5 mV.

Table 1 summarizes the following electrochemical parameters from the SAMs of each EAM: apparent formal potential (E^0),²⁰ peak splitting between anodic and cathodic waves (ΔE_p), full-width at half-maximum (ΔE_{fwhm}), ratio of anodic and cathodic peak currents (i_{pa}/i_{pc}), and ferrocene surface coverage (Γ_{Fc}). The Γ_{Fc} values were estimated from the charge passed for the oxidation of ferrocene during the anodic sweep.²¹ For reference, the generally accepted theoretical maximum Γ_{Fc} for a hexagonally closed-packed ferrocenyl-alkanethiolate monolayer (Fc diameter = 6.6 Å) on gold is 4.5 × 10⁻¹⁰ mol·cm⁻².²² Further, the entropically determined ideal reversible one-electron faradaic response for identical, noninteracting redox groups in a SAM is defined by a symmetric waveshape with ΔE_{fwhm} of 90.6 mV and ΔE_p = 0 at 25 °C.⁸

Representative CVs of the resulting SAMs from each EAM are shown in Figure 2. In all cases, a single set of symmetric faradaic peaks were observed corresponding to one-electron redox processes of immobilized ferrocenes. Repeated CV scans did not influence peak appearance suggesting SAM stability. To evaluate monolayer integrity under analogous conditions for maleimide-terminated SAM

(20) The apparent formal potential E^0 is defined as the mean of the anodic (E_{pa}) and cathodic (E_{pc}) peak potentials.

(21) Surface coverages were estimated using $\Gamma_{Fc} = Q_{Fc}/nFA$, where Q_{Fc} is the charge passed for the oxidation of ferrocene during the anodic sweep (obtained by integrating the faradaic peak current vs. time), n is the number of electrons involved in the electron transfer process ($n = 1$ for Fc/Fc⁺ redox couple), F is the Faraday constant, and A is the experimental surface area of the electrode.

(22) Rowe, G. K.; Carter, M. T.; Richardson, J. N.; Murray, R. W. *Langmuir* **1995**, *11*, 1797.

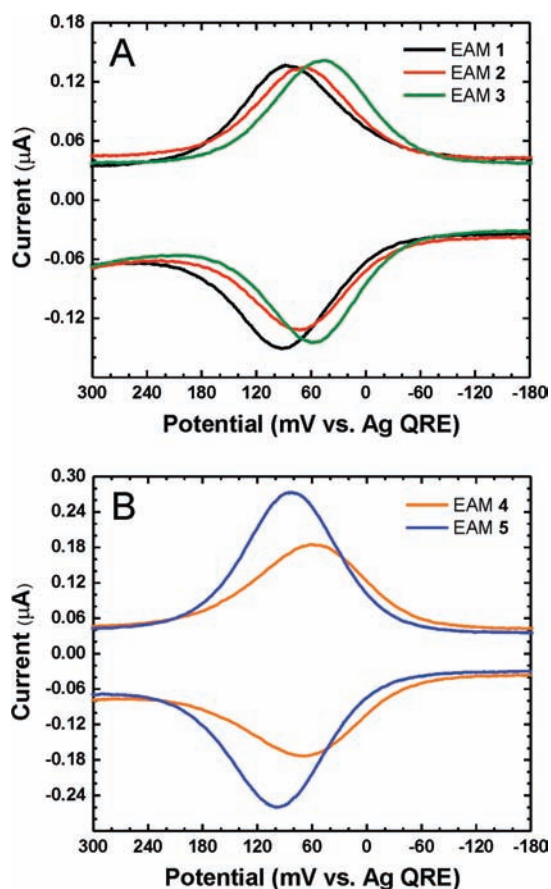


Figure 2. Overlaid cyclic voltammograms (vs Ag QRE) obtained for dilute SAMs of (A) EAMs 1–3 and (B) EAMs 4–5 in aqueous 1.0 M LiClO₄. Scan rate 10 V·s⁻¹, Pt wire counter electrode, gold working electrode area = 4.91 × 10⁻⁴ cm².

biofunctionalization,^{9a} SAMs were exposed to aqueous 2-mercaptoethanol (0.5 mM, 2 h). Importantly, less than 1% loss of faradaic current was observed indicating negligible EAM exchange under these conditions (see Supporting Information). The experimental ΔE_p values obtained were relatively small (ranging from 6 to 17 mV) even at high scan rate, the i_{pa}/i_{pc} values were near unity, and the anodic peak currents increased linearly with scan rate (see Supporting Information) confirming surface confinement of ferrocene in the SAMs.⁸

The CVs from SAMs of asymmetric EAMs 1–3 displayed similar peak shapes with $E^{0'}$ values ranging from 52 to 87 mV (Figure 2A). The differences in $E^{0'}$ values may be attributed to variable ferrocene microenvironments in the diluted SAMs. The corresponding ΔE_{fwhm} values were in close agreement and slightly larger than ideal, suggesting

structural inhomogeneity of ferrocenes in the SAMs and/or ferrocenyl interaction with the interfacial charge of the double layer.²³ The average Γ_{Fc} values estimated for EAMs 1–3 were ~6–7% of the theoretical maximum surface coverage for a ferrocenyl alkanethiolate SAM on gold.²² These values are in close agreement with the 5% mole fractions of ferrocenyl components in the mixed SAM-deposition solutions. It is noteworthy that the Γ_{Fc} from EAM 3 is comparable to EAMs 1 and 2 despite the branched nature of the ferrocene-maleimide headgroup.

SAMs of branched EAMs 4 and 5 displayed CVs with $E^{0'}$ values of 62 and 87 mV, respectively (Figure 2B). Significantly, the ΔE_{fwhm} value from EAM 4 was the largest in the series at 134 mV while EAM 5 had a peak shape closest to ideal with a ΔE_{fwhm} of 108 mV. With only seven atoms separating the branching methine carbon in EAM 4 from the anchoring disulfide group, it is reasonable to assume that peak broadening is due to some structural inhomogeneity of ferrocenes in the SAM with (C₁₁S)₂ and (HOC₁₁S)₂ diluents.^{23a} In contrast, the closer to ideal ΔE_{fwhm} of EAM 5 implies minimal lateral interaction between redox centers in the SAM possibly due to the increased bridge length. Interestingly, the Γ_{Fc} values for EAMs 4 and 5 were ~11 and 15% of the theoretical maximum coverage, respectively. These significantly higher Γ_{Fc} values compared to EAMs 1–3 may be due to different SAM packing geometries and/or faster adsorption kinetics of the bipodal EAM anchors compared to the symmetric disulfide diluents.

In summary, a series of ferrocene-based EAMs containing maleimide and disulfide groups in different asymmetric and branched architectures have been designed and synthesized. Mixed SAMs of the EAMs on gold with symmetric disulfide diluents were characteristic of stable electroactive monolayers as evidenced by CV. Further studies aimed at biofunctionalization of these EAM scaffolds in SAMs toward the fabrication of integrated electrochemical biosensors are ongoing.

Acknowledgment. We acknowledge the Integrated Molecular Structure Education and Research Center (IMSERC) at Northwestern University for instrument use (NMR, MS).

Supporting Information Available: Abbreviations used, experimental procedures, and spectra for new compounds. This material is available free of charge via the Internet at <http://pubs.acs.org>.

OL101180R

(23) (a) Calvente, J. J.; Andreu, R.; Molero, M.; Lopez-Perez, G.; Dominguez, M. *J. Phys. Chem. B* **2001**, *105*, 9557. (b) Smith, C. P.; White, H. S. *Anal. Chem.* **1992**, *64*, 2398.